Equilibrium configurations of Pearl vortices in narrow strips

Eric Bronson, Martin P. Gelfand, and Stuart B. Field
Department of Physics, Colorado State University, Fort Collins, Colorado 80523, USA
(Received 17 November 2005; published 3 April 2006)

We have calculated the equilibrium configurations of Pearl vortices in narrow strips of superconducting thin films, within the large thin-film penetration depth limit of the London theory. The results are reminiscent of those for Abrikosov vortices in thin films with parallel magnetic fields. The calculations are compared with recent experimental results of Stan, Field, and Martinis [Phys. Rev. Lett. **92**, 097003 (2004)]. Reasonable agreement with experiment requires refinement of the theoretical model to account for pinning and an often-neglected contribution to the vortex core energy in thin films identified by Pearl.

DOI: 10.1103/PhysRevB.73.144501 PACS number(s): 74.78.−w, 74.25.Qt, 74.20.De, 74.25.Ha

I. INTRODUCTION

The characteristics of the mixed state have significant differences for superconducting samples with small dimensions perpendicular to the applied field when compared to the corresponding phenomena in bulk type-II superconductors. For an infinite sheet of thickness W with the magnetic field directed parallel to the surface of the sheet, Abrikosov[1,2] showed that the equilibrium critical field for vortices to appear in the sheet is $2\Phi_0 \ln(W/\xi)/\pi W^2$, for $\xi \ll W \ll \lambda$. (As usual, Φ_0 is the superconducting flux quantum, ξ is the coherence length, and λ is the bulk penetration depth.) The vortices appear first in the center of the sheet, and as the field increases the spacing between them decreases until a critical field is reached at which the line of vortices "buckles," forming two rows. Increasing the field further leads to a sequence of first-order transitions, at "matching fields," in which the number of vortices in a unit cell of the vortex lattice increases by one and the vortex density jumps. Detailed theoretical calculations of vortex lattice structures with this geometry of film and field have been carried out by Carter[3] and Carneiro[4] and Luzhbin,[5] while experimental studies that reveal transitions between vortex structures (though in multilayer systems rather single films) have been carried out by Guimpel *et al.*[6] and Brongersma *et al.*[7] A qualitative feature of the theory, remarked on by Abrikosov, is that the vortex density has infinite slope at the critical field, because the interaction between vortices falls off exponentially at large intervortex distances.

The present work is motivated by a recent experimental study of vortices in narrow, thin films of niobium, carried out by Stan, Field, and Martinis[8,9] (SFM), in which Hall probe microscopy was used to image films, patterned into strips of width W, subject to *perpendicular* magnetic fields. In this configuration of superconductor and magnetic field, the superconductor develops *Pearl* vortices[10] rather than *Abrikosov* vortices. SFM offered the first experimental results for equilibrium vortex density as a function of magnetic field B. They found that the threshold field for vortex entry B_c scaled roughly as $1/W^2$, just as for confined Abrikosov vortices. However, the vortex density exhibited apparently linear behavior in $B-B_c$ above threshold. The slopes of the vortex density versus B data were consistent with $1/\Phi_0$, as is the case for an infinite thin film with a perpendicular field. There were also vortices appearing at fields below the nominal B_c, which were attributed to pinning.

There have been other studies of the physics of vortices in superconducting films with small lateral dimensions. The possibility of equilibrium measurements on vortices was established by Finnemore and co-workers,[11,12] in demonstrating that, sufficiently close to T_c, vortices spontaneously leave pinning sites and wander through the film. Many transport measurements that reflect the interactions between vortices in thin films which have been patterned into parallel narrow strips of low-pinning superconductor between wider strips of strong-pinning material have been carried out following the study of Pruymboom *et al.*;[13] following in that tradition is the recent work by Grigorieva *et al.*[14] on vortices in a single narrow thin film strip, which showed that pushing on vortices in one part of the strip led to vortex flow many intervortex lengths away. What sets SFM apart is its focus on equilibrium properties in a well-defined narrow thin film strip geometry; this leads to the consideration of several fundamental matters which are not relevant in other experiments.

The equilibrium threshold field for vortices in narrow thin film strips has been addressed theoretically by both Clem[15] and Likharev.[16] (Clem argues that a more relevant threshold field would be associated with metastability rather than equilibrium, but see SFM for a discussion of why the equilibrium condition seems to be more appropriate for that experiment.) Their arguments are based on calculations, within the London theory, of the Gibbs free energy change associated with the addition of a single vortex to the center of an otherwise vortex-free strip of width W and thickness d. Clem's expression for this is

$$\Delta G = -\frac{\Phi_0 B W^2}{16\pi\Lambda} + \frac{\Phi_0^2}{8\pi^2\Lambda}\ln(2W/\pi\xi), \tag{1}$$

where $\Lambda = 2\lambda^2/d$ is the thin-film penetration depth and it is assumed that $\Lambda \gg W \gg \xi$. (Likharev's expression differs only in the constant factors in the logarithm.) The first term is associated with the interaction of the vortex with the screening currents in the film, while the second term arises from the change in the currents due to the vortex; we shall refer to

these as the Meissner term and the self-energy, respectively. Clem's derived Eq. (1) by considering the forces on a vortex and integrating.

Alternatively, Eq. (1) may be derived by an energetic approach,[17] in which one notes that $\Phi_0 W^2/16\pi\Lambda$ is the magnetic moment of a vortex in the center of the strip and that the self-energy is the free energy of such a vortex in zero external field, both of which have been calculated within the London theory by Kogan.[18] This perspective on Eq. (1) is more helpful when considering possible corrections to that formula, such as those we will suggest in Sec. VI.

Setting $\Delta G=0$ yields

$$B_c = \frac{2\Phi_0}{\pi W^2}\ln(2W/\pi\xi). \tag{2}$$

For later convenience let us define the scale of the vortex self-energy

$$\varepsilon_0 = \Phi_0^2/8\pi^2\Lambda, \tag{3}$$

which has the value $\varepsilon_0 \approx 0.13$ eV in SFM.

The only theoretical work that touches on the density of vortices for $B > B_c$ is that of Maksimova,[19] who treats vortices in a mean-field manner by considering only the variation of the currents in the film in the direction across the strip and ignoring variations along its length. This leads to a result for ΔG for adding a vortex to the center of the strip which is a simple extension of Eq. (1),

$$\Delta G = -\frac{\Phi_0 B}{4\pi\Lambda}\left(\frac{W}{2} - \frac{N\Phi_0}{2BL}\right)^2 + \varepsilon_0 \ln(2W/\pi\xi), \tag{4}$$

in which N is the number of vortices in a strip of length L. Setting this to zero leads to the equilibrium vortex density

$$\frac{N}{LW} = [B - (B_c B)^{1/2}]/\Phi_0. \tag{5}$$

For $B \gg B_c$ this gives $N/LW \sim B/\Phi_0$, while just above threshold $N/LW \approx (B-B_c)/2\Phi_0$, that is, the slope is smaller than observed experimentally by a factor of 2.

The problem is now clear: For bulk samples or thin films with fields parallel to the surface, theory and experiment show that just above the threshold for vortex penetration the vortex density increases very quickly with field (theoretically, with infinite slope) due to the exponentially weak vortex-vortex interactions at large distances. However, for narrow thin film strips with perpendicular fields, both the experiments of SFM and the mean field approach of Maksimova seem to imply a finite slope in the vortex density as a function of B just above threshold, of order $1/\Phi_0$. We will begin by considering this problem theoretically using approaches which have previously been applied to the study of confined Abrikosov vortices. In Sec. II, we construct the Gibbs potential for the narrow strip, including interactions between vortices. This serves as the basis for all subsequent calculations.

We find in Sec. III that the qualitative features of confined Abrikosov vortices are reproduced in the theoretical analysis for confined Pearl vortices. In particular, the vortex density exhibits an infinite slope at B_c. A detailed comparison of the preceding theoretical calculations with the experiments and the mean-field approach is offered in Sec. IV, where the differences between the theory and the experimental results at low vortex density are clearly exhibited.

All of the theoretical calculations up to this point treat superconductors without any pinning sites. In Sec. V the effects of vortex pinning are approximately modeled in a manner suitable for the low vortex density regime. Pinning can markedly change the how the vortex density depends on field. However, pinning cannot increase the threshold field, and since that is already underestimated by Eq. (2) in two of the three samples studied by SFM, some other physical mechanism must be invoked. This motives us to introduce in Sec. VI another expression for the vortex self-energy, following Pearl,[17] to account for the contribution of the vortex cores. Due to theoretical uncertainties we treat this expression as containing an adjustable parameter. With the freedom to adjust several model parameters we are able to fit some experimental data reasonably well, as shown in Sec. VII but interesting questions remain.

Section VIII offers a summary and conclusions.

II. THE GIBBS POTENTIAL

The derivation of a general expression for the Gibbs potential for an arbitrary configuration of Pearl vortices in a thin film of width W is fairly straightforward, following the work of Kogan.[18] In constructing a solution within London theory of the current density associated with an arbitrarily located vortex, he essentially produced an explicit formula for the interaction energy between two vortices when $\Lambda \gg W$. This condition is satisfied for any strip at temperatures sufficiently close to T_c, and in SFM it is valid for the two narrower samples they studied.

Let us establish a coordinate system with the z axis perpendicular to the film, the y axis directed along its length, and the x axis across the strip, which is bounded by $-W/2 \leqslant x \leqslant W/2$. We will set $G=0$ for the vortex-free film. The expression for G for a *single* vortex at an arbitrary position x, generalizing Eq. (1), was already found by Clem[15] and Likharev[16] and has the form

$$G_1 = -\frac{\Phi_0 B}{16\pi\Lambda}(W^2 - 4x^2) + \varepsilon_0 \ln\left(\frac{2W}{\pi\xi}\cos\frac{\pi x}{W}\right) \tag{6}$$

again taking Clem's factors in the logarithm.

The interaction free energy between vortices with coordinates (x_1, y_1) and (x_2, y_2) is proportional to Kogan's current potential, his Eq. (35), which may be written in the manifestly symmetric form

$$G_2 = \varepsilon_0 \ln\left[\frac{\cosh\pi(y_i - y_j)/W + \cos\pi(x_i + x_j)/W}{\cosh\pi(y_i - y_j)/W - \cos\pi(x_i - x_j)/W}\right]. \tag{7}$$

For $|y_2 - y_1| \gg W$, G_2 decays as $\exp(-\pi|y_2 - y_1|/W)$. For comparison, recall that in an infinite film the interaction decays as $1/r$ for $r \gg \Lambda$.

III. VORTEX CONFIGURATIONS BY FREE-ENERGY MINIMIZATION

The problem now is to find the lowest G configuration of vortices for a given externally applied field. Since we are considering strips in which the length L is much greater than all other length scales, it is appropriate to minimize the Gibbs potential density $g \equiv G/L$ and to explore vortex configurations which are periodic in y. It is useful to introduce the dimensionless vortex density $n \equiv NW/L$.

For fields just above B_c, the intervortex spacing is large and G_1 forces the vortices to lie along the center line of the strip. Since G_2 is repulsive, the vortices lie the same distance W/n apart and the unit cell of the vortex lattice contains just one vortex. Placing that vortex at (0,0) leads to the expression $g(n,B)=nG_1+n\Sigma_{i>0}G_2[(0,0),(0,iW/n)]$. The sum over the two-body terms is dominated by the first term. Setting $\partial g/\partial n=0$ and solving for the leading behavior yields $n=-\pi/\ln(B-B_c)$: just as in the case of confined Abrikosov vortices, the vortex density increases with infinite slope at the threshold field.

To go beyond the behavior at threshold, we turned to numerical evaluation of g and its minimization by Powell's method. With increasing field, configurations with more vortices in a unit cell become competitive in free energy. We explored the same types of configurations as have been considered for confined Abrikosov lattices,[3,4] namely, "slices" of a triangular lattice, in which the vortices have some freedom of movement but are not permitted to break the symmetries that remain in the slice. Some resulting configurations are sketched in Fig. 1, where we also present a plot of $n(B)$ for $W/\xi=30$, which is appropriate for the 10 μm strips in SFM. Note that there is one type of configuration corresponding to every positive number m of vortices in a unit cell. The number of variables with respect to which g must be minimized is $(1+m)/2$ for odd m and $1+m/2$ for even m.

Our findings concerning the vortex structure and density as a function of B are qualitatively the same as previous results for Abrikosov vortices.[3,4] Similar results are found for narrow Wigner crystal strips,[20] and would probably be found for almost any repulsive pointlike objects in a strip geometry. As the field increases, the vortices are eventually forced off the center line into the "two-row" configuration shown on the left in Fig. 1(b); this is manifested in the plot of $n(B)$ by the kink at $B_{c2}=2.48B_c$ and $n=2.43$. This is a classical second order phase transition, with the vortex displacement from the center line serving as the order parameter. Subsequent transitions to configurations with more vortices per unit cell, at fields denoted $B_{c3}, B_{c4}, \ldots$, are first order. We will denote the arrangement of vortices between B_{cn} and $B_{c(n+1)}$ as an "n-row" pattern. We did not calculate the domains of metastability for these phases since they do not bear directly on the experiment of SFM.

Analogous calculations were carried out for $W/\xi=300$ and 5, for comparison with the 100 and 1.6 μm strips examined by SFM. The results for the former look very much like those in Fig. 1. However, for $W/\xi=5$ there are no transitions out of the one-row pattern. In such narrow strips B_c is much greater, and hence, the interaction with the Meissner currents is stronger relative to the intervortex forces.

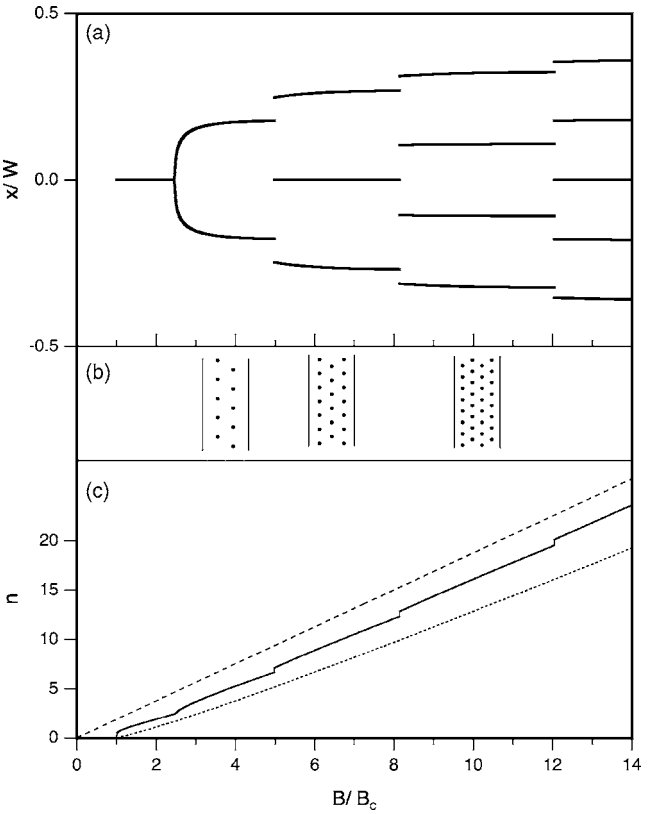

FIG. 1. Vortex configurations and density as a function of B/B_c, for $W/\xi=30$. (a) Transverse coordinates of the vortices. (b) Illustrations of the vortex configurations for several values of B. (c) Vortex density according to the present calculations (solid line) and Maksimova's free energy (dotted line). The dashed line corresponds to $n=BW^2/\Phi_0$.

We also carried out unconstrained minimizations of g by overdamped molecular dynamics starting from random initial configurations, to provide further assurance that the calculations described above (which can be characterized as constrained minimization) found configurations that were global free-energy minima. We will omit details of these calculations and summarize the results. For fields below B_{c2}, the unconstrained minimization always converged to the expected one-row configuration. For $B_{c2}<B<B_{c3}$, they usually gave vortex configurations matching those predicted by the constrained minimization, but there were also some results that deviated from a periodic arrangement. In those cases a vortex would be trapped near the center of the strip, causing the other vortices nearby to be pushed towards the edges. The disturbance in the vortex lattice was localized: within several W, the vortices returned to a nearly periodic two-row pattern. Such vortex configurations with defects were always higher in g than the periodic ones. For $B>B_{c3}$, local minima in g proliferated and the unconstrained minimizations never converged to periodic patterns; and again the resulting values of g always exceeded those of the periodic configurations found previously.

IV. ASSESSMENT OF THE THEORY

Now we directly address the questions that motivated this work. On the purely theoretical side, we may compare the

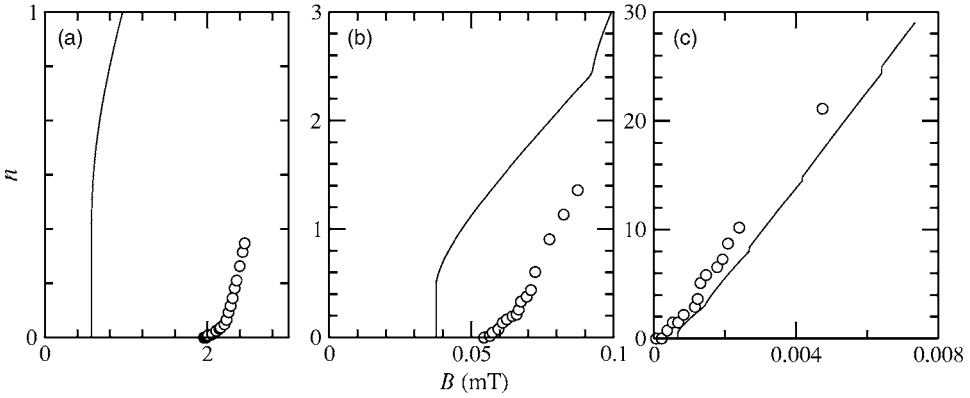

FIG. 2. Data of Stan, Field, and Martinis (see Ref. 8) (circles) and the corresponding theoretical results (solid lines) for (a) $W=1.6$ μm, $W/\xi=5$, (b) $W=10$ μm, $W/\xi=30$, and (c) $W=100$ μm, $W/\xi=300$.

result for $n(B)$ that follows from Maksimova's mean-field treatment of vortices, Eq. (5), with our findings: see Fig. 1(c). There are marked differences near B_c, where as noted earlier the slope of $n(B)$ is infinite in the proper treatment but is $W^2/2\Phi_0$ in the mean-field treatment. There are also significant differences at larger fields. A straight line—without any further term that diverges as $B\to\infty$—fits the calculations of Sec. III quite well for $B\gtrsim 2B_c$. Fitting $n(B)$ displayed in Fig. 1(c) gives a slope of $0.96W^2/\Phi_0$. Doing the same with the corresponding calculations for $W/\xi=300$ yields the somewhat smaller slope $0.87W^2/\Phi_0$. The mean-field calculation yields $n(B)=(B-\sqrt{BB_c})W^2/\Phi_0$, so dn/dB approaches its large-B limit rather slowly. It is evident in Fig. 1(c) that the difference between the exact and mean-field calculations increases with increasing B (except just below some of the vortex structure transitions).

In order to facilitate a comparison with the experimental results, in Fig. 2 we have taken the data from Ref. 8 and plotted it together with the theoretical results, using the published experimental estimates of the parameters.

The most obvious disagreements between theory and experiment, already noted by SFM, are in the values of B_c: the theory underestimates it by a factor of about 4 in the 1.6 μm strips and overestimates it by about 50% in the 100 μm strips. For the 1.6 μm strips, W/ξ may be too small for the theory to be quantitatively reliable. For the 100 μm strips the condition $W\ll\Lambda$ is not satisfied, since SFM estimated $\Lambda=24$ μm. Although a full accounting of the effects of finite Λ is beyond the scope of this work, a few remarks are in order. A calculation by Fetter[21] for thin-film disks showed that on decreasing Λ from five times the diameter to half the diameter, B_c increased by 10%. Thus the finite Λ should have only a negligible effect on B_c for the 1.6 and 10 μm strips; for the 100 μm strips it should have a small effect but leads to a greater discrepancy between theory and experiment for B_c.

The 1.6 μm data is all in the low vortex density regime, for which the theory predicts $n(B)$ to be nearly vertical, and which is not consistent with the data. The 10 μm data at low vortex densities are also qualitatively inconsistent with the theory, but for $n\gtrsim 0.6$ its slope is reasonably consistent with the theoretical result. Data at larger values of magnetic field would have been very interesting to see. The 100 μm data is too sparse at low vortex density to compare with the theory, but for larger values of density and field the theory and experiment are in reasonable agreement. The experimental data are too scattered to reveal any of the vortex configuration transitions evident in the theoretical curve.

We suggest that some of the features of the data that cannot be accounted for yet, such as the finite slope at low vortex density ($n\lesssim 0.6$) for the 1.6 and 10 μm strips and the unexpectedly low value of the critical field in the 100 μm strips, are due to pinning. The following section will address that matter.

V. PINNING

So far we have assumed that the superconducting films were structurally and chemically perfect. In real materials this is never true, and in fact disorder that leads to particularly favored locations for vortices, that is, *pinning*, is necessary for the critical current to be nonzero when vortices are present. Modeling pinning, in the present context, amounts to choosing a particular ensemble of functions $V(x,y)$ to add to G_1; one might take, for example, parabolic "dimples."[22] (Vortex entanglement and related phenomena are not possible when $d<\xi$, so variations of the pinning potential in z can be averaged.)

While it is certain that pinning has effects on the vortex configurations and mean density at all fields, we are especially interested in understanding if pinning can account for the experimentally observed behavior low values of n, where the theory for systems without pinning places all vortices along the strip center line and $n(B)$ rises much more rapidly with field than observed by SFM. Thus we have constructed a model for pinning which is appropriate in that regime and makes possible calculations which are computationally less intensive than would be necessary for a full treatment.

In this model the vortices are allowed to lie only along $x=0$ at discrete values of y separated by W/M; for most calculations we set $M=100$. Each of these "sites" has an associated energy $-E$. For most of the sites $E=0$. The remainder are "pinning sites" with E drawn uniformly from 0 to $E_{\max}$. Other choices of distribution could be made; we will comment on this matter later. The average number of pinning sites in a length W will be denoted ρ, so the fraction of sites which are pinning sites is ρ/M.

For a given set of parameters and realization of pinning, approximate ground state configurations for a strip of length $40W$ with lengthwise periodic boundaries are determined by

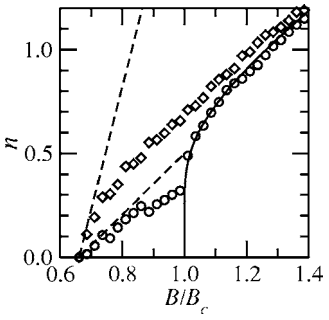

FIG. 3. Vortex density for $W/\xi=30$, $E_{\max}/\varepsilon_0=1$, at pinning site densities ρ of zero (solid line), 0.5 (circles), and 2 (diamonds). The uncertainties in the Monte Carlo calculations are approximately or less than the height of the symbols. The dashed lines neglect intervortex interactions, as described in the text.

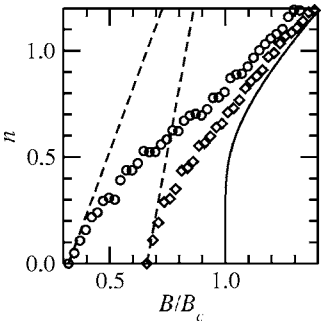

FIG. 4. Vortex density for $W/\xi=30$, pinning site density $\rho=2$, and scaled maximum pinning energies $E_{\max}/\varepsilon_0$ of zero (solid line), 1 (diamonds), and 2 (circles). The uncertainties in the Monte Carlo calculations are approximately or less than the height of the symbols. The dashed lines neglect intervortex interactions.

simulated annealing with a Metropolis Monte Carlo algorithm, following an exponential cooling schedule. Allowed moves are addition of a vortex to an empty site, removal of a vortex from a filled site, and displacement of a vortex to an empty adjacent site. Results for n are averaged over ten realizations of pinning.

(Note that the "cooling" carried out in these calculations is very different from experimental cooling: in the calculations the vortex interactions are independent of temperature. In fact, the Monte Carlo calculations start at temperatures of order ε_0/k_B, which are well above the superconducting transition temperature.)

Our present aim is to gain insight into how varying the disorder model parameters $E_{\max}$ and ρ affects the vortex density. We begin with two analytic calculations. The threshold field in the presence of pinning, which we will refer to as B_c^{pin}, is determined by subtracting $E_{\max}$ from the right side of Eq. (1) and setting $\Delta G=0$. This yields

$$B_c^{\text{pin}}/B_c = 1 - E_{\max}/\varepsilon_0 \ln(2W/\pi\xi). \tag{8}$$

The slope of $n(B)$ at B_c^{pin} is determined entirely by the pinning site density and the probability distribution of pinning energies, since just above B_c^{pin} the mean intervortex distance is large and interactions between vortices can be neglected. If those interactions are neglected completely, then, for a uniform distribution of pinning energies, $n(B)$ forms straight lines from $n(B_c^{\text{pin}})=0$ to $n(B_c)=\rho$.

Let us now examine some numerical calculations. In Fig. 3 we show results for two nonzero values of ρ, fixing $W/\xi=30$ and $E_{\max}=\varepsilon_0$. Those two data sets exhibit the same threshold field, as expected since that depends on the maximum strength of pinning rather than the density of pinning sites. The dashed lines (the lower one corresponding to the $\rho=0.5$, the higher to $\rho=2$) are the results in the absence of intervortex interactions, so effects of vortex-vortex interactions are evident in the deviations of the Monte Carlo data from those lines. For the present set of parameters, interactions begin to noticeably affect the density when the vortices are on average $3W$ apart. At that distance $G_2=3\times10^{-4}\varepsilon_0$, so it is somewhat surprising that interaction effects are evident then. Randomness in the distances between pinning sites as well as the pinning energies must underlie this behavior.

For fields exceeding B_c by as little as 10%, pinning has only a modest effect on the vortex density. It is interesting to see that for "low" pinning densities such as 0.5, where an extrapolation of the low-n part of the $n(B)$ data intersects the clean-system $n(B)$ curve, there is a distinctive "kink" where those two meet, as the Monte Carlo data follows the clean-system theory remarkably well beyond that point. For "high" pinning densities there is no corresponding feature at B_c, just a decrease in slope when n is large enough that intervortex interactions become significant.

In Fig. 4 the effects of varying the maximum pinning energy are illustrated. The most obvious result of increasing $E_{\max}$, all other things being equal, is the expected downward shift in B_c^{pin}. Above B_c, where the Monte Carlo data essentially follows the clean-system theory, it appears that increasing $E_{\max}$ as well as ρ (as seen on the previous figure) leads to slightly increased n values, but the effect is modest. If the pinning site density is low (such as $\rho=0.5$) the effect of $E_{\max}$ on n above B_c is even weaker, as shown in Fig. 5.

VI. RECONSIDERATION OF THE SINGLE-VORTEX FREE ENERGY

The fact that the experimental values of the threshold field for vortex entry in the 1.6 and 10 μm strips are too large in comparison with the theoretical results shown in Fig. 2 cannot be accounted for by pinning: B_c^{pin} is alway less than B_c. If

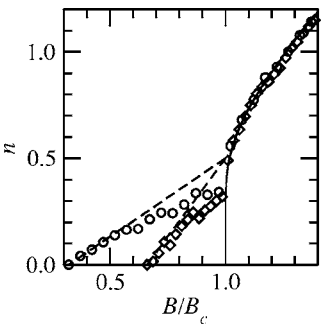

FIG. 5. Same as Fig. 4, except $\rho=0.5$.

the experimental results are taken at face value, there must be something missing in Eq. (1). Either an additional contribution to the vortex self-energy or a reduction in the magnetic moment would have the effect of increasing B_c. In fact, both types of corrections to Eq. (1) exist.

Equation (1) is obtained within London theory. The vortex core is treated as pointlike for the calculation of the magnetic moment of the vortex, since the moment is finite even with the divergent current density at the vortex center. For the calculation of the self-energy, the current density is set to zero within ξ of the vortex center.

For a vortex in an infinite film, Pearl[17] applied a variational approximation to Ginzburg-Landau theory to derive an expression for the vortex self-energy, namely

$$\varepsilon_0\left[\ln\frac{\Lambda}{r_c}+\frac{1}{24}\left(\frac{r_c}{\xi}\right)^2\right], \tag{9}$$

where r_c is the core radius, outside of which the order parameter is taken to be constant. The corresponding result within London theory is just the first term, and if one sets $r_c=\xi$ then the second term is just a (very small) constant. For a vortex along the center line of a thin film strip, it seems natural to replace the first term by $\ln(2W/\pi r_c)$ and again set $r_c=\xi$. The contributions to the vortex self-energy beyond London theory (such as the condensation energy of the core) would then seem to be insignificant since 1/24 is just 1.5% of $\ln(2W/\pi\xi)=2.95$ for $W/\xi=30$ (10 μm strips).

However, in addition to the expression (9), Pearl also found that the core radius r_c for a thin-film vortex is *not* the coherence length, but rather, within the same approximation

$$r_c=(12\Lambda\xi^2)^{1/3}. \tag{10}$$

Although Pearl emphasized that r_c for a thin-film vortex was not much different than in bulk (in contrast with the strikingly different behaviors of the current far from the core), for our purposes the ratio $r_c/\xi=(12\Lambda/\xi)^{1/3}=9.7$ is significantly different from unity. We are thus led to propose that the self energy for a thin-film strip has the form

$$\varepsilon_0\left[\ln\frac{2W}{\pi\xi}-\ln\frac{r_c}{\xi}+\frac{1}{24}\left(\frac{r_c}{\xi}\right)^2\right] \tag{11}$$

provided that $(12\Lambda\xi^2)^{1/3}\ll W/2$ so that the core structure is not significantly altered by the strip geometry. Note that for SFM $(12\Lambda\xi^2)^{1/3}=3.1$ μm, so for the $W=1.6$ μm strips this condition is strongly violated. Then we cannot use Eq. (11) for the self-energy. Instead, a full Ginzburg-Landau analysis is required, which might be done by generalizing Brandt's calculations for films.[23] For the $W=10$ μm strips, the condition barely holds. If we treat Eqs. (11) and (10) as exact then the ratio of the last two terms to the first in Eq. (11) is 65%. Going beyond London theory thus yields a 65% increase in the self-energy, which leads directly to a 65% increase in B_c over that given by Eq. (2). For the $W=100$ μm strips, there is a 30% increase.

Let us now turn to the vortex magnetic moment. The magnetic moment of a Pearl vortex in the center of a narrow strip within London theory is $(\Phi_0/16\pi\Lambda)W^2$ [cf. Eq. (1)]. Assuming that the currents within the vortex core are unaffected by the strip geometry, they contribute $(\Phi_0/16\pi\Lambda)r_c^2$ to the magnetic moment. If those currents are simply set to zero, there is a correction factor $1-(r_c/W)^2$ to the magnetic moment, and if one takes $r_c=\xi$ then the correction factor is clearly negligible for the $W=10$ μm strips. However, as we have just seen, it is preferable to use Eq. (10). One should also note that in Pearl's approximation the current density varies as r^2 for $r<r_c$, so the correction factor becomes $1-\frac{1}{2}(r_c/W)^2$. For the $W=10$ μm strips, $\frac{1}{2}(r_c/W)^2\approx 0.05$: this is just small enough that it is reasonable to neglect. For the $W=100$ μm strips the correction to the magnetic moment is insignificant, but for the $W=1.6$ μm strips one sees again that a full Ginzburg-Landau treatment is called for.

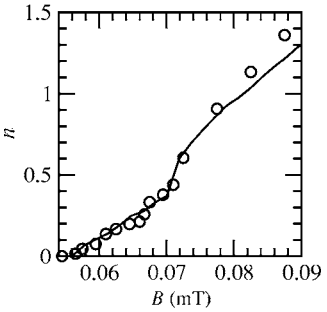

FIG. 6. The $W=10$ μm data of SFM (circles) together with theoretical calculations (line, Monte Carlo uncertainties suppressed for clarity) for $\rho=0.6$, $E_{\max}/\varepsilon_0=1.1$, $r_c/\xi=10.7$.

VII. FITTING THE SFM DATA

Let us now see to what degree we can account for the data of SFM by including pinning and the improved self-energy Eq. (11) in the analysis. The $W=10$ μm data cover the most interesting range in n, so we start with that. We take ρ, $E_{\max}/\varepsilon_0$, and r_c/ξ as fitting parameters. We fit r_c/ξ rather than fixings its value with Eq. (10) because of the approximations inherent in both (10) and (11).

Looking at the data in Fig. 2(b), the pinning site density should be low, since there is a clear *increase* in slope at about 0.07 mT. (Compare Fig. 5, with low pinning density, to Fig. 4, with high density.) The experimental data directly yields $B_c^{\rm pin}=0.056$ mT$=2.7\Phi_0/W^2$. We carried out Monte Carlo calculations for several sets of parameter values consistent with that constraint, and what we consider to be the best representation of the data is shown in Fig. 6. The uncertainties in the fitting parameters are roughly 0.2 in r_c/ξ and with correlated variations of about 0.1 in $E_{\max}/\varepsilon_0$ and ρ. Note that the fitted r_c/ξ is in reasonable agreement with the value 9.7 expected on the basis of Eq. (10). The theoretical curve ends up giving one a rather different impression of the data than one gets from the SFM paper, in which the data for $B\geqslant 0.07$ mT is fit with a straight line that is extrapolated to $n=0$ to estimate B_c. Here, the drop in n with decreasing field at about 0.07 mT is interpreted as the beginning of the sudden drop one expects to see in the absence of pinning, but which is masked by pinning for $n<0.4$.

The linearity of the experimental data for $n\lesssim 0.4$ is consistent with the assumption of a uniform distribution of pin-

ning energies. However, none of the good fits were able to pass through the two data points at the largest values of B. This may be a consequence of the approximate pinning model, which should become less reliable as n increases. It could also be due to the incipient breakdown of the London theory for vortex-vortex interactions, since r_c is not much less than $W/2$.

In order to extend the above results for the $W=10$ μm strips to the other strips, we must consider how the parameters of the pinning model should vary with W. Recall that ρ is the number of pinning sites, taken to lie on the strip center line, in a segment of length W. If all the pinning sites in the experimental samples really were along the center line then changing W would change ρ by the same factor and leave $E_{\max}$ unchanged. But that assumption of the model was introduced just for calculational convenience. It is clear that the effective values of ρ and $E_{\max}$ for the model calculations should be somewhat less than those values for narrower strips, and somewhat greater for wider strips; a more detailed analysis requires further assumptions concerning the pinning sites and is not needed for our present purposes.

For the $W=1.6$ μm strips we have already pointed out that the London theory is inapplicable, and one can even see evidence for this in qualitative aspects of the data [see Fig. 2(a)] related to the intervortex interactions. The pinning site density should be smaller by about a factor of 1.6/10 than for the $W=10$ μm strips, which puts the $W=1.6$ μm strips well into the low pinning density regime ($\rho \approx 0.1$). One then expects linear behavior in $n(B)$ between the vortex entry threshold ($B=B_c^{\mathrm{pin}}, n=0$) up to $n \approx \rho$ (at which point B is presumably B_c), which does in fact hold in the experimental data. But one also expects this to be followed, on increasing B, by an abrupt jump up to $n \approx 0.5$—which is notably lacking.

Finally, consider the $W=100$ μm strips. For these one expects to have a large pinning site density, perhaps $\rho \approx 6$ or greater, and pinning energies $E_{\max}/\varepsilon_0 \approx 1$ or greater. A detailed comparison between theory and experiment like that in Fig. 6 is not possible since the model calculations with pinning are restricted to small n, where the data is very sparse. The calculations also omit the effects of a finite Λ, except insofar as it sets the energy scale ε_0, but as remarked earlier we expect that to give only small corrections. Taking into account the self-energy beyond the London theory, Eq. (11), shifts the no-pinning theoretical curve in Fig. 2(c) to the right by 2×10^{-4} mT, which would be barely visible on that graph. Including pinning should then improve the agreement between theory and experiment. Matching the experimental B_c requires accepting a value of $E_{\max}/\varepsilon_0$ as large as 5. It is not clear how to square this with the results for the 10 μm strips, but a high density of strong pinning sites might account for the consistently larger numbers of vortices found in the experiments compared with the theoretical prediction for clean systems shown in Fig. 2(c), particularly at $B > 0.002$ mT.

VIII. CONCLUSIONS

We have carried out an analysis within the London theory of the equilibrium configurations of Pearl vortices in narrow thin-film strips. In the absence of pinning, the results for the vortex configurations and density as a function of magnetic field bear a strong resemblance to the corresponding results for Abrikosov vortices in thin films with magnetic fields parallel to the film surface. There are notable differences with the vortex density found using Maksimova's approximate treatment[19] in which variations in the sheet current density along the strip length are neglected, and also with that found in the experimental work of SFM,[8] particularly near the threshold field for vortex entry.

When pinning is included in the analysis, it is possible to account for the finite slope of $n(B)$ seen experimentally at threshold. However, to construct a reasonable fit to the SFM data for 10 μm strips, it is necessary to go somewhat beyond London theory by incorporating Pearl's[17] Ginzburg-Landau analysis of the core structure and free energy of thin-film vortices. Pearl's analysis implies that when $\Lambda \gg \xi$ the core radius r_c of Pearl vortices can be appreciably greater than the coherence length, and for the thin films considered by SFM the effect is about a factor of 10. Thus SFM provides, as far as we are aware, the first experimental support for this particular little-known aspect of Pearl's pioneering study of thin-film vortices. For SFM's 1.6 μm strips the core diameter, as calculated in an infinite film, is about four times greater than the strip width, and so the London theory is inapplicable. A full Ginzburg-Landau treatment for such extremely narrow strips may be worthwhile.

ACKNOWLEDGMENTS

We would like to thank O. Jonsson for technical assistance and A. Fetter for correspondence. This work was supported in part by the National Science Foundation through Grant No. DMR-0308699.

[1] A. A. Abrikosov, Sov. Phys. JETP **19**, 988 (1964).
[2] A. A. Abrikosov, *Fundamentals of the Theory of Metals* (North-Holland, Amsterdam, 1988).
[3] C. Carter, Can. J. Phys. **47**, 1447 (1969).
[4] G. Carneiro, Phys. Rev. B **57**, 6077 (1998).
[5] D. A. Luzhbin, Phys. Solid State **43**, 1823 (2001).
[6] J. Guimpel, L. Civale, F. de la Cruz, J. M. Murduck, and J. K. Schuller, Phys. Rev. B **38**, 2342 (1988).
[7] S. H. Brongersma, E. Verweij, N. S. Koeman, D. G. de Groot, R. Griessen, and B. I. Ivlev, Phys. Rev. Lett. **71**, 2319 (1993).
[8] G. Stan, S. B. Field, and J. M. Martinis, Phys. Rev. Lett. **92**, 097003 (2004).
[9] G. Stan, Ph.D. thesis, Colorado State University, Fort Collins, CO, 2005.
[10] J. Pearl, Appl. Phys. Lett. **5**, 65 (1964).
[11] J. Sok and D. K. Finnemore, Phys. Rev. B **50**, 12770 (1994).

[12] D. Kouzoudis, M. Breitwisch, and D. K. Finnemore, Phys. Rev. B **60**, 10508 (1999).
[13] A. Pruymboom, P. H. Kes, E. van der Drift, and S. Radelaar, Phys. Rev. Lett. **60**, 1430 (1988).
[14] I. V. Grigorieva, A. K. Geim, S. V. Dubonos, K. S. Novoselov, D.Y. Vodolozov, F. M. Peeters, P. H. Kes, and M. Hesselberth, Phys. Rev. Lett. **92**, 237001 (2004).
[15] J. R. Clem (unpublished).
[16] K. K. Likharev, Radiophys. Quantum Electron. **6**, 722 (1972).
[17] J. Pearl, Ph.D. thesis, Polytechnic Institute of Brooklyn, Brooklyn, NY, 1965.
[18] V. G. Kogan, Phys. Rev. B **49**, 15874 (1994).
[19] G. M. Maksimova, Phys. Solid State **40**, 1607 (1998).
[20] G. Piacente, I. V. Schweigert, J. J. Betouras, and F. M. Peeters, Phys. Rev. B **69**, 045324 (2004).
[21] A. L. Fetter, Phys. Rev. B **22**, 1200 (1980).
[22] C. Reichhardt, C. J. Olson, and F. Nori, Phys. Rev. B **57**, 7937 (1998).
[23] E. H. Brandt, Phys. Rev. B **71**, 014521 (2005).